University of Wollongong

Research Online

1-1-2013

Impact of humic acid fouling on membrane performance and transport of pharmaceutically active compounds in forward osmosis

Ming Xie
University of Wollongong, mx504@uowmail.edu.au

Long D. Nghiem
University of Wollongong, longn@uow.edu.au

William E. Price
University of Wollongong, wprice@uow.edu.au

Menachem Elimelech
Yale University

Recommended Citation

Impact of humic acid fouling on membrane performance and transport of pharmaceutically active compounds in forward osmosis

Abstract

The impact of humic acid fouling on the membrane transport of two pharmaceutically active compounds (PhACs) - namely carbamazepine and sulfamethoxazole - in forward osmosis (FO) was investigated. Deposition of humic acid onto the membrane surface was promoted by the complexation with calcium ions in the feed solution and the increase in ionic strength at the membrane surface due to the reverse transport of NaCl draw solute. The increase in the humic acid deposition on the membrane surface led to a substantial decrease in the membrane salt (NaCl) permeability coefficient but did not result in a significant decrease in the membrane pure water permeability coefficient. As the deposition of humic acid increased, the permeation of carbamazepine and sulfamethoxazole decreased, which correlated well with the decrease in the membrane salt (NaCl) permeability coefficient. It is hypothesized that the hydrated humic acid fouling layer hindered solute diffusion through the membrane pore and enhanced solute rejection by steric hindrance, but not the permeation of water molecules. The membrane water and salt (NaCl) permeability coefficients were fully restored by physical cleaning of the membrane, suggesting that humic acid did not penetrate into the membrane pores.

Keywords

performance, fouling, acid, transport, humic, impact, pharmaceutically, active, membrane, compounds, osmosis, forward

Disciplines

Engineering | Science and Technology Studies

Publication Details

Impact of humic acid fouling on membrane performance and transport of pharmaceutically active compounds in forward osmosis

Water Research

Revised: 6th May 2013

Ming Xie [1], Long D. Nghiem [1,*], William E. Price [2], and Menachem Elimelech [3]

[1] Strategic Water Infrastructure Laboratory, School of Civil, Mining and Environmental Engineering, University of Wollongong, Wollongong, NSW 2522, Australia

[2] Strategic Water Infrastructure Laboratory, School of Chemistry, University of Wollongong, Wollongong, NSW 2522, Australia

[3] Department of Chemical and Environmental Engineering, Yale University, New Haven, CT 06520-8286, USA

---

* Corresponding author: Long Duc Nghiem, Email: longn@uow.edu.au; Ph +61 2 4221 4590

16   **Abstract**

17   The impact of humic acid fouling on the membrane transport of two pharmaceutically
18   active compounds (PhACs) – namely carbamazepine and sulfamethoxazole – in forward
19   osmosis (FO) was investigated. Deposition of humic acid onto the membrane surface was
20   promoted by the complexation with calcium ions in the feed solution and the increase in ionic
21   strength at the membrane surface due to the reverse transport of NaCl draw solute. The
22   increase in the humic acid deposition on the membrane surface led to a substantial decrease
23   in the membrane salt (NaCl) permeability coefficient but did not result in a significant
24   decrease in the membrane pure water permeability coefficient. As the deposition of humic
25   acid increased, the permeation of carbamazepine and sulfamethoxazole decreased, which
26   correlated well with the decrease in the membrane salt (NaCl) permeability coefficient. It is
27   hypothesized that the hydrated humic acid fouling layer hindered solute diffusion through the
28   membrane pore and enhanced solute rejection by steric hindrance, but not the permeation of
29   water molecules. The membrane water and salt (NaCl) permeability coefficients were fully
30   restored by physical cleaning of the membrane, suggesting that humic acid did not penetrate
31   into the membrane pores.

1. Introduction

A large proportion of the world's population lives in areas with severe water shortages. This problem is being further exacerbated by urbanisation, population growth, and climate change. As a result, over the last few decades, significant efforts have been made to develop innovative treatment processes that utilise alternative water sources such as seawater and reclaimed wastewater in order to ensure a secure and reliable supply of clean drinking water that is independent of the hydrological cycle. Notable progress can be seen in the field of membrane filtration technologies. For example, seawater desalination and wastewater reuse by reverse osmosis (RO) and nanofiltration (NF) membrane filtration have been widely used to augment the freshwater supply in many parts of the world (Elimelech and Phillip 2011, Shannon et al. 2008). Forward osmosis (FO), which is a membrane-based filtration process, is still emerging but has the potential to advance water and wastewater treatment (Cath et al. 2006, Zhao et al. 2012). Compared to the NF and RO processes, FO has a much smaller fouling propensity (Mi and Elimelech 2008). Instead of hydraulic pressure, FO utilises the osmotic pressure of a highly concentrated draw solution as the driving force to transfer water from the feed solution to the draw solution through a dense polymeric membrane. As a result, FO can potentially be employed as a pre-treatment for the NF/RO processes (Hoover et al. 2011, Shaffer et al. 2012, Yangali-Quintanilla et al. 2011) or in combination with a membrane bioreactor (Achilli et al. 2009, Alturki et al. 2012) to extract clean water from wastewater and other alternative water sources.

The occurrence of chemicals of emerging concern, particularly pharmaceutically active compounds (PhACs), in wastewater and secondary treated effluent at trace levels is a major issue associated with wastewater reuse, particularly when intended for potable purposes (Basile et al. 2011, Carballa et al. 2004, Schwarzenbach et al. 2006). Several recent studies have investigated the removal of PhACs by FO. These studies reveal that the removal mechanisms of PhACs by FO membranes are governed by several factors, including membrane interfacial properties (Jin et al. 2012a), physicochemical properties of the solutes (Alturki et al. 2013, Hancock et al. 2011b, Valladares Linares et al. 2011) and solution chemistry (Xie et al. 2012b). However, the current state-of-the-art understanding of PhAC rejection behaviour in the FO process is still limited. In particular, little is known about the impact of membrane fouling on the rejection of PhACs.

The effect of membrane fouling on the rejection of PhACs has been investigated extensively in NF and RO processes. These studies suggest that membrane fouling influences

the rejection of PhACs via modification of membrane surface charge (Plakas et al. 2006, Xu et al. 2006), pore blockage (Nghiem and Hawkes 2007) or cake enhanced concentration polarization (Ng and Elimelech 2004, Vogel et al. 2010), thereby either improving or reducing their rejection. By drawing on these well-established mechanisms in NF and RO processes, several studies have also been initiated to shed light on the impact of membrane fouling on the rejection of PhACs in FO. Hancock et al. (2011b) observed that rejection of PhACs by the FO process substantially increased when the membrane was fouled by wastewater effluent in a pilot-scale setup. Valladares Linares et al. (2011) proposed that the fouling layer altered the charge and hydrophobicity of the FO membrane surface, thereby enhancing the rejection of ionic and neutral PhACs. Jin et al. (2012b) highlighted the enhanced membrane sieving effect by membrane fouling when they compared the rejections of boron and arsenate by an alginate-fouled FO membrane.

In FO, for a non-ideal membrane with less than 100% solute rejection, the water flux is coupled with a reverse permeation of the draw solute. Recently, several studies were conducted to understand this mechanism (Hancock and Cath 2009, Xie et al. 2012a) and to quantify this bi-directional mass transfer (Hancock et al. 2011a, Phillip et al. 2010, Yong et al. 2012). Specifically, membrane fouling could be affected by the reverse permeation of draw solutes. Boo et al. (2012) reported that reverse permeation of draw solutes promoted colloidal aggregation, which enhanced membrane fouling and reduced fouling reversibility by simple physical cleaning. As a result, it is of practical interest to understand the role of reverse permeation of draw solutes on membrane fouling and its associated effect on the rejection of PhACs.

The aim of this study is to investigate the impact of humic acid fouling on the membrane permeation of two model PhACs (i.e. sulfamethoxazole and carbamazepine) in forward osmosis. Fouling and PhAC flux through the membrane were investigated under different calcium ion concentrations and a variety of draw solutions. Key membrane properties, and forward hydrogen ion and reverse salt fluxes were measured to elucidate the impact of humic acid fouling on the permeation of PhACs. Mechanisms accounting for the impact of humic acid fouling on PhAC permeation were systematically proposed and delineated.

2. Materials and methods

2.1. Forward osmosis membrane

An asymmetric cellulose-based membrane specifically designed for FO applications was supplied by Hydration Technology Innovations (Albany, OR). While detailed composition of the membrane is proprietary, it is believed that it has a dense cellulose triacetate active layer embedded in a polyester mesh. Further details about this FO membrane are available elsewhere (Cath et al. 2006, McCutcheon and Elimelech 2008).

2.2. Determination of water and salt (NaCl) permeability coefficients

Water permeability coefficient (A) and salt (NaCl) permeability coefficient (B) were determined using a standard method recently established by Cath et al. (2013). Briefly, the measurement was conducted in RO mode using a laboratory scale cross-flow filtration system. Prior to each measurement, the membrane was compacted at 15 bar using deionised water for at least 12 hours until a constant permeate water flux had been obtained. The water permeability coefficient was determined by dividing the pure water permeate flux obtained at 10 bar (145 psi) using deionised water as the feed by the applied hydraulic pressure. NaCl was then added to the feed solution to obtain a concentration of 2000 mg/L in order to determine the salt (NaCl) permeability coefficient at 10 bar (145 psi). The RO system was stabilised for two hours before the permeate water flux (J_w^{NaCl}) was recorded and feed and permeate samples were taken to determine the observed NaCl rejection value (R_o). The observed salt (NaCl) rejection, R_o, was calculated from the difference between the bulk feed (c_b) and permeate (c_p) salt concentrations, $R_o = 1 - c_p/c_b$. The B value was determined from (Cath et al. 2013):

$$B = J_w^{NaCl}\left(\frac{1-R_o}{R_o}\right)\exp\left(-\frac{J_w^{NaCl}}{k_f}\right) \qquad (1)$$

where k_f is the mass transfer coefficient for the cross-flow channel of the RO membrane cell.

The mass transfer coefficient (k_f) was experimentally determined using the film theory (Sutzkover et al. 2000):

$$k_f = \frac{J_{salt}}{\ln\left[\frac{\Delta P}{\pi_b - \pi_p}\left(1 - \frac{J_{salt}}{J_w}\right)\right]} \qquad (2)$$

4

where π_p and π_b are the osmotic pressures of the permeate and 2000 mg/L NaCl feed solution, respectively; ΔP is the applied pressure; and J_w and J_{salt} are the pure water flux and the water flux of the 2000 mg/L NaCl feed solution, respectively.

To measure the membrane pure water and salt (NaCl) permeability coefficient in the presence of a humic acid fouling layer, the membrane was pre-fouled with a feed solution of 50 mg/L humic acid and a calcium concentration varying between 0 and 4 mM at 10 bar (145 psi) for 10 hours. The membrane pure water and salt (NaCl) permeability coefficients were then measured using the same protocol as described above.

2.3. Zeta potential measurement

The membrane zeta potential was determined using a streaming current electrokinetic analyser (SurPASS, Anton Paar GmbH, Austria). The zeta potential was calculated from the measured streaming potential data using the Fairbrother-Mastin method (Elimelech et al. 1994). Streaming potential measurement was conducted in a background electrolyte solution containing 10 mM KCl. The same electrolyte solution was used to flush the cell thoroughly prior to automatic pH titration using either hydrochloric acid (1 M) or potassium hydroxide (1 M). All measurements were performed at room temperature (approximately 22 ºC), which was monitored by the temperature probe of the instrument.

Prior to the zeta potential measurement, the humic acid fouled membranes were dried in a desiccator. The dried membranes were then soaked in Milli-Q water for 24 hours prior to the measurement. A small amount of humic acid was released into the solution and the rest was stable on the membrane surface. This procedure effectively prevents the removal of the humic acid fouling layer due to hydrodynamic shear stress during the streaming potential measurement (Simon et al. 2011).

2.4. Chemical reagents

Analytical grade sulfamethoxazole and carbamazepine were purchased from Sigma–Aldrich (St. Louis, MO) and used as model PhACs. They are active ingredients of pharmaceutical products and have been frequently detected at trace levels in secondary treated effluents and sewage-impacted water bodies (Schwarzenbach et al. 2006). Their molecular structures and key physicochemical properties are summarised in Table 1. At the experimental pH of 6.5, sulfamethoxazole is negatively charged due to the dissociation of its amine functional group, while carbamazepine is neutral. A stock solution of 2 g/L was

155 obtained by dissolving these two compounds in pure methanol. The stock solution was stored

156 at -18 °C in the dark and was used within one month.

157 **[Table 1]**

158   Humic acid (Sigma-Aldrich, St. Louis, MO) was selected as a model organic foulant.

159 Humic acid stock solution (10 g/L) was prepared by dissolving the humic acid powder as

160 received in Milli-Q water and adjusting the pH to 8.2 with NaOH to ensure complete

161 dissolution. The stock solution was stored in a sterilized amber glass bottle at 4 °C and was

162 used within one month.

2.5. *Forward osmosis setup*

163

164   A bench-scale flat-sheet cross-flow FO system described in our previous publication

165 (Xie et al. 2012b) was used (Supplementary Data, Figure S1). The membrane cell had two

166 identical and symmetrical flow chambers with a length, width and channel height of 130, 95,

167 and 2 mm, respectively. The membrane sample was inserted between the two chambers to

168 separate the feed solution from the draw solution. The total effective membrane area for mass

169 transfer was 123.5 cm^2.

170   Two variable speed gear pumps (Micropump, Vancouver, WA) were used to circulate

171 the feed and draw solutions. Flow rates of the feed and draw solutions were monitored using

172 two rotameters and kept constant at 1 L/min (corresponding to a cross-flow velocity of 9

173 cm/s). The draw solution reservoir was placed on a digital balance (Mettler-Toledo Inc.,

174 Hightstown, NJ) and weight changes were recorded by a computer to calculate the permeate

175 flux. The conductivity of the draw solution was continuously measured using a conductivity

176 probe (Cole-Parmer, Vernon Hills, IL). To maintain constant draw solution concentration, a

177 peristaltic pump was regulated by a conductivity controller to intermittently dose a small

178 volume of a concentrated draw solution (6 M NaCl or 4 M MgSO$_4$, depending on the type of

179 draw solution) into the draw solution reservoir (control accuracy was ± 0.1 mS/cm). The

180 concentrated draw solution makeup reservoir was also placed on the same digital balance.

181 This setup ensured that the transfer of liquid between the two reservoirs did not interfere with

182 the measurement of permeate water flux and that the system could be operated at a constant

183 osmotic pressure driving force during the experiment. Manual control of draw solution

184 concentration was applied when neutral glucose and urea were used as draw solutes in the FO

185 experiment. A concentrated glucose (6 M) or urea (6 M) solution was manually added into

186 the draw solution reservoir every two hours to avoid the dilution of the draw solution and the

187 decline of osmotic pressure driving force.

2.6. Membrane fouling protocol

189   In all FO experiments, the initial volumes of feed and draw solutions were 4 L and 1

190 L, respectively. A new membrane sample was used for each experiment. Mass concentrations

191 of humic acid and each PhAC in the feed solution (20 mM NaCl and 1 mM $NaHCO_3$) were

192 50 mg/L and 500 µg/L, respectively. The concentration of $CaCl_2$ varied from 0 to 4 mM in

193 the feed solution. Approximate 2 mL of feed and draw solution samples were taken at

194 specific time intervals for HPLC analysis to determine the concentration of the PhACs, and

195 an 8-mL aliquot sample of the feed was also collected at the same time to measure the humic

196 acid concentration.

197   Because of the dilution of draw solution and the concentration of feed solution, PhAC

198 permeation (P_s) through the membrane was proposed and employed as an indicator of the

199 impact of the humic acid fouling layer on the permeation of PhACs. P_s was calculated by

200 taking into account the draw solution dilution using a mass balance. Because the PhAC

201 permeate concentration in the FO process is diluted by the draw solution, the actual

202 (corrected) concentration of the target solute, $C_{s(t)}$, can be obtained by taking into account the

203 dilution using a mass balance:

204
$$C_{s(t)} = \frac{C_{ds(t)}V_{ds(t)} - C_{ds(t-1)}V_{ds(t-1)}}{V_{w(t)}}$$
(3)

205 where $V_{w(t)}$ is the permeate volume of water to the draw solution at time t; $V_{ds(t-1)}$ is the

206 volume of draw solution at time (t-1); $V_{ds(t)}$ is the volume of draw solution at time t; $C_{ds(t)}$ is

207 the measured concentration of target solute in the draw solution at time t; and $C_{ds(t-1)}$ is the

208 measured concentration of target solute in the draw solution at time (t-1). Subsequently, P_s is

209 calculated using the actual permeate concentration after accounting for water recovery (i.e.,

210 25% in all experiments), yielding:

211
$$P_s = \frac{C_{ds(t)}V_{ds(t)}}{C_{f(0)}V_{f(0)}}100\%$$
(4)

212 where $C_{f(0)}$ and $V_{f(0)}$ are the concentrations of the target solute in the feed solution and the

213 volume of feed solution at *zero* time.

214   The reduction in PhAC permeation (P_{sr}) was used to evaluate the impact of the humic
215   acid fouling layer on the permeation of PhACs:

216
$$P_{sr} = \frac{P_{s-clean} - P_{s-fouled}}{P_{s-clean}} 100\% \qquad (5)$$

217   where $P_{s-clean}$ and $P_{s-fouled}$ are the permeation of PhACs through the clean and humic acid
218   fouled FO membrane, respectively.

219   The reverse flux of draw solute J_{salt} and forward hydrogen ion flux J_H in the FO
220   process were determined using the mass balance calculation:

221
$$J_H \text{ or } J_{salt} = \frac{(C_t V_t - C_0 V_0)}{At} \qquad (6)$$

222   where C_0 and C_t are the concentrations of the draw solute or hydrogen ion in the feed at
223   time 0 and t, respectively; V_0 and V_t are the volumes of the feed at time 0 and t, respectively;
224   A is the membrane area, and t is the operating time of the FO experiment. Draw solute
225   concentrations of NaCl and MgSO$_4$ in the feed solution were determined by measuring
226   electric conductivity and using the calibration curves of NaCl and MgSO$_4$, while those of
227   glucose and urea were determined using total organic carbon (TOC) measurement. The
228   concentrations of glucose and urea were determined using a TOC analyser (TOC-V$_{CSH}$,
229   Shimadzu, Kyoto, Japan). The hydrogen ion concentration in the feed was determined by the
230   measurement of feed solution pH value.

231   The amount of humic acid deposited on the membrane surface was determined using
232   the mass balance calculation:

$$m_{HA} = \frac{(C_{t-HA} V_t - C_{0-HA} V_0)}{A}$$

233    $\qquad (7)$

234   where C_{0-HA} and C_{t-HA} are the concentrations of humic acid in the feed at time 0 and t,
235   respectively. The concentration of humic acid was determined by UV absorbance
236   measurement at 254 nm using a UV-Vis Spectrophotometer (UV-1700, Shimadzu, Kyoto,
237   Japan). A linear calibration curve with a coefficient of determination (R^2) greater than 0.99
238   between humic acid concentration and UV_{254} absorbance was obtained within the
239   concentration range used in this study.

2.7. Analytical methods

241   A Shimadzu HPLC system (Shimadzu, Kyoto, Japan), equipped with a Supelco Drug

242 Discovery C18 column (with a diameter, length, and pore size of 4.6 mm, 150 mm, and 5 µm,

243 respectively) and a *UV–Vis* detector, was used to measure the concentration of

244 carbamazepine and sulfamethoxazole in the feed and draw solution samples. The detection

245 wavelength was 280 nm. Milli-Q water buffered with 25 mM KH_2PO_4 and acetonitrile were

246 used as the mobile phase at a flow rate of 1 mL/min. The sample injection volume was 50

247 µL. Calibration yielded a linear curve with a coefficient of determination (R^2) above 0.99.

248 Carbamazepine and sulfamethoxazole analysis was carried out immediately upon the

249 conclusion of each experiment. The limit of quantification for carbamazepine and

250 sulfamethoxazole under these conditions was approximately 10 µg/L.

3. Results and discussion

3.1. *Impact of fouling on membrane properties*

253   Deposition of humic acid onto the membrane surface was insignificant when the feed

254 solution contained 50 mg/L of humic acid and no calcium (Figure 1). As calcium

255 concentration in the feed solution increased from 0 to 4 mM, the amount of humic acid

256 deposited on the membrane surface increased significantly from 1.35 to 7.22 mg/cm². The

257 influence of calcium concentration on the deposition of humic acid onto the membrane

258 surface can be attributed to the complexation between calcium and humic acid molecules (Mi

259 and Elimelech 2008, Nghiem et al. 2008). In fact, visual observation of the membrane

260 samples at the end of each experiment confirmed the proportional increase in humic acid

261 deposition with respect to the increase in calcium concentration (Supplementary Data, Figure

262 S2).

263   **[Figure 1]**

264   The formation of a humic acid fouling layer on the membrane surface did not result in

265 significant decrease in the membrane pure water permeability coefficient; however, it led to a

266 substantial decrease in the membrane salt (NaCl) permeability coefficient (Figure 2). It is

267 noteworthy that the membrane salt (NaCl) permeability coefficient was measured in RO

268 mode after the membrane was pre-fouled with humic acid at an initial permeate flux of 6.5

269 L/m²h (which is also the flux used in the FO experiments). Under this condition, the

270 deposition of humic acid on the membrane surface could be visually confirmed, but water

271   flux decline was negligible (Supplementary Data, Figure S2) and the water flux behaviour

272   obtained in the RO mode was similar to that in the FO mode. Therefore, the membrane pure

273   water and salt (NaCl) permeability coefficients of the humic acid fouled membrane obtained

274   in RO mode can be used to assess the impact of the humic acid cake layer on membrane

275   performance in the FO process.

276   **[Figure 2]**

277   Possessing a large number of free hydroxyl and carboxylic functional groups, the humic

278   acid layer can be highly hydrated (Wang et al. 2001). These hydrated humic acid molecules

279   can block the membrane pores and enhance solute rejection by steric hindrance, which

280   reduces solute transport through the membrane. In the FO process, the transport of water

281   through the membrane is driven mostly by diffusion. This is also true in the RO mode when

282   the permeate flux is sufficiently low. Unlike convective transport, the diffusion of water

283   molecules through the membrane pores is not adversely influenced by a hydrated humic acid

284   layer on the membrane surface, because the hydrated humic acid layer provides more

285   available sites, which facilitate the diffusion of water molecules and thereby, compensate for

286   the blockage of membrane pores (Cohen-Tanugi and Grossman 2012). As a result, the humic

287   acid fouling layer reduced the membrane solute (NaCl) permeability coefficient but did not

288   induce any significant impact on the membrane water permeability coefficient (Figure 2).

289   *3.2. Impact of fouling on water and reverse salt fluxes*

290   Generally, the presence of the humic acid fouling layer did not result in any

291   significant FO water flux decline (Figure 3). Using 0.5 M NaCl as the draw solution, the

292   water flux decreased slightly from 6.5 to 5.1 L/m^{2}h within the first hour of filtration and

293   remained stable at 5.1 L/m^{2}h throughout the remaining duration of the experiment. Without

294   humic acid in the feed (denoted as 'clean matrix'), the water flux decline was insignificant.

295   Similarly, no significant water flux decline could be observed even when a discernible humic

296   acid fouling layer formed on the membrane surface at high calcium ion concentrations. This

297   negligible flux decline can be explained by the relatively low water permeate flux and low

298   humic acid fouling layer resistance under the experimental conditions. At a low water

299   permeate flux, the external and internal concentration polarizations are negligible and thus

300   the impact of a humic acid cake layer on permeate flux is expected to be insignificant.

301   Furthermore, the estimated humic acid layer resistance (R_c) was less than 1% of the

302   membrane intrinsic resistance (Supplementary Data, Appendix A). Our results are consistent

303 with a recent study by Parida and Ng (2013) who also reported limited water flux decline

304 when they examined FO fouling using a feed matrix containing up to 50 mg/L organic

305 foulant and 5 mM calcium.

306 **[Figure 3]**

307 The formation of a humic acid fouling layer rendered the membrane surface more

308 negatively charged. In addition, the membrane surface became more negatively charged as

309 calcium concentration in the feed solution increased (Figure 4). The increase in membrane

310 negative surface charge could reduce the transport of feed and draw solution ions in the

311 forward and reverse directions. Consequently, at the experimental pH value of 6.5, as the

312 calcium concentration in the feed solution increased from 0 to 4 mM, the membrane zeta

313 potential changed from -5 to -38 mV (Figure 4) and the reverse draw salt (NaCl) flux

314 decreased by more than ten-fold, from 3.49 to 0.22 g/m^2h (Figure 1). Ion transport in the FO

315 process is bi-directional (Hancock et al. 2011a); thus, a decrease in the reverse draw salt

316 (NaCl) flux also led to a decrease in the forward hydrogen ion flux as observed in Figure 1. It

317 is likely that the reverse flux of Cl^- was hindered by an enhanced electrostatic interaction with

318 the more negatively charged humic acid fouling layer. To maintain the electroneutrality of the

319 feed solution, the forward diffusion of hydrogen ions was coupled with the reverse permeate

320 of draw solution Na^+ (Hancock and Cath 2009, Xie et al. 2012b). Therefore, the forward

321 hydrogen ion flux also decreased with the decrease in the reverse draw salt flux as the

322 concentration of calcium increased from 0 to 4 mM.

323 **[Figure 4]**

324 *3.3. Impact of fouling on PhAC permeation*

325 *3.3.1 Role of calcium and humic acid fouling*

326 Permeation of the neutral carbamazepine decreased substantially from 23% under

327 clean membrane conditions to 14% when humic acid was introduced to a feed solution that

328 did not contain calcium (Figure 5). The molecular width of carbamazepine is 0.529 nm

329 (Table 1) while the membrane pore diameter is 0.74 nm (Xie et al. 2012a). Thus, it is possible

330 that the hydrated humic acid fouling layer could have hindered solute transport through the

331 membrane pore, thereby reducing the permeation of carbamazepine as humic acid fouling

332 occurred. Hindrance of carbamazepine permeation caused by the hydrated humic acid fouling

333 layer was further enhanced as calcium was introduced to the feed solution, (which also led to

334 an increase in the deposition of humic acid on the membrane surface as reported in section
335 3.1). Indeed, carbamazepine permeation decreased further to 3% as the calcium concentration
336 in the feed solution increased from 0 to 4 mM (Figure 5).

337 The molecular width of sulfamethoxazole is slightly larger than that of
338 carbamazepine. More importantly, at pH 6.5, both the membrane and more than 90% of
339 sulfamethoxazole molecules are negatively charged (Figure 4). Thus, in addition to steric
340 hindrance, electrostatic interaction also plays an important role in the rejection of this
341 compound (Xie et al. 2012b). As a result, permeation of the charged sulfamethoxazole was
342 considerably smaller than that of the neutral carbamazepine. The permeation of the
343 negatively charged sulfamethoxazole decreased from 10% in the clean matrix to 6.1% in the
344 humic acid matrix with no calcium in solution (Figure 5). The permeation of
345 sulfamethoxazole decreased further to 1.2% as the deposition of humic acid on the membrane
346 surface increased due to the introduction of 4 mM calcium to the feed solution. It is
347 noteworthy that reduction in the permeation of both carbamazepine and sulfamethoxazole
348 correlates very well with the decrease in the membrane salt (NaCl) permeability coefficient
349 reported in section 3.1. Coefficients of determination (R^2) of the linear regression between the
350 membrane salt (NaCl) permeability coefficient and the reduction in carbamazepine and
351 sulfamethoxazole permeation were 0.996 and 0.997, respectively.

352 **[Figure 5]**

353 *3.3.2 Role of reverse draw salt flux*

354 To provide further insight into the impact of the humic acid fouling layer on the
355 passage of carbamazepine and sulfamethoxazole through the FO membrane, $MgSO_4$, urea,
356 and glucose were also used as the draw solutes, in addition to NaCl, to obtain a range of
357 reverse draw solute fluxes (Figure 6). In a clean matrix, reverse draw solute flux could hinder
358 the forward diffusion of neutral solutes, through a phenomenon known as 'retarded forward
359 diffusion', thereby reducing their permeation through the FO membrane (Xie et al. 2012a). In
360 agreement with the retarded forward diffusion phenomenon, permeation of neutral
361 carbamazepine in the clean matrix is inversely proportional to the reverse draw solute flux
362 (Figure 6), which is in the order of urea < NaCl < glucose < $MgSO_4$ (Figure 7) when these
363 draw solutes were used in FO experiments.

364 Different types and degrees of reverse draw solute flux resulted in varying amounts of
365 humic acid deposited on the membrane surface. The amount of humic acid deposited on the

366   membrane surface for the fouling experiments with the four types of draw solutes was in the

367   following order: $NaCl > MgSO_4 \approx urea \approx glucose$ (Figure 6). Reverse transport of ionic NaCl

368   draw solute likely elevated the localized ionic strength in the fouling layer and led to further

369   aggregation of humic acid foulant, thereby promoting the deposition of humic acid (Tang et

370   al. 2011).

371   Varying deposition of humic acid on the membrane surface using four types of draw

372   solutes led to differing reductions in the permeation of carbamazepine and sulfamethoxazole.

373   The reductions occurred in the following order: $NaCl > MgSO_4 \approx urea \approx glucose$ (Figure 7),

374   which was the same as the order of draw solutes observed when measuring the amount of

375   humic acid deposition on the membrane surface (Figure 6). This observation was consistent

376   with our hypothesis that the hydrated humic acid fouling layer hindered feed solute transport

377   through the membrane pores, thereby reducing their permeation.

378   **[Figure 6]**

379   **[Figure 7]**

380   *3.4. PhAC permeation after physical cleaning of the membrane*

381   Membrane cleaning was conducted by increasing the cross-flow velocity from 9 to 18

382   cm/s. Because of the low hydraulic resistance and loose structure of the humic acid cake

383   layer, which is a characteristic of the fouling layer in FO (Mi and Elimelech 2008), it is not

384   surprising that the humic acid cake layer was fully removed by the increase in the shearing

385   rate. This physical cleaning restored the permeation of carbamazepine and sulfamethoxazole

386   as well as the reverse salt (NaCl) flux to those of the virgin (clean) membrane (Figure 8). The

387   reversible fouling behaviour observed here confirms a weak adhesion of humic acid to the

388   membrane surface (Mi and Elimelech 2008) and suggests that humic acid did not penetrate

389   into the membrane pores.

390   **[Figure 8]**

4. Conclusion

392   Results reported here indicate that calcium in the feed solution promoted the

393   deposition of humic acid onto the membrane surface. Higher deposition of humic acid was

394   also observed when NaCl was used as the draw solute due to an increase in ionic strength at

395   the membrane interface in comparison to $MgSO_4$, glucose, and urea, which exhibited a

396   negligible reverse solute flux or are organic based. The increase in humic acid deposition on

the membrane surface led to a substantial decrease in the membrane salt (NaCl) permeability coefficient but did not result in a significant decrease in the membrane pure water permeability coefficient. The decrease in carbamazepine and sulfamethoxazole permeation as the deposition of humic acid increased, which correlated well with the decrease in the membrane salt (NaCl) permeability coefficient. It is hypothesized that the hydrated humic acid fouling layer hindered solute transport through the membrane pores and enhanced steric hindrance, but not the diffusion of water. Results reported here also indicate that the humic acid did not penetrate into the membrane pores.

5. Acknowledgments

6. References

Achilli, A., Cath, T.Y., Marchand, E.A. and Childress, A.E. (2009) The forward osmosis membrane bioreactor: A low fouling alternative to MBR processes. Desalination 239(1–3), 10-21.

Alturki, A., McDonald, J., Khan, S.J., Hai, F.I., Price, W.E. and Nghiem, L.D. (2012) Performance of a novel osmotic membrane bioreactor (OMBR) system: Flux stability and removal of trace organics. Bioresource Technology 113, 201-206.

Alturki, A.A., McDonald, J.A., Khan, S.J., Price, W.E., Nghiem, L.D. and Elimelech, M. (2013) Removal of trace organic contaminants by the forward osmosis process. Separation and Purification Technology 103, 258-266.

Basile, T., Petrella, A., Petrella, M., Boghetich, G., Petruzzelli, V., Colasuonno, S. and Petruzzelli, D. (2011) Review of Endocrine-Disrupting-Compound Removal Technologies in Water and Wastewater Treatment Plants: An EU Perspective. Industrial & Engineering Chemistry Research 50(14), 8389-8401.

Boo, C., Lee, S., Elimelech, M., Meng, Z. and Hong, S. (2012) Colloidal fouling in forward osmosis: Role of reverse salt diffusion. Journal of Membrane Science 390–391, 277-284.

Carballa, M., Omil, F., Lema, J.M., Llompart, M.a., García-Jares, C., Rodríguez, I., Gómez, M. and Ternes, T. (2004) Behavior of pharmaceuticals, cosmetics and hormones in a sewage treatment plant. Water Research 38(12), 2918-2926.

Cath, T.Y., Childress, A.E. and Elimelech, M. (2006) Forward osmosis: Principles, applications, and recent developments. Journal of Membrane Science 281(1–2), 70-87.

Cath, T.Y., Elimelech, M., McCutcheon, J.R., McGinnis, R.L., Achilli, A., Anastasio, D., Brady, A.R., Childress, A.E., Farr, I.V., Hancock, N.T., Lampi, J., Nghiem, L.D., Xie, M. and Yip, N.Y. (2013) Standard Methodology for Evaluating Membrane Performance in Osmotically Driven Membrane Processes. Desalination 312, 31-38.

434 Cohen-Tanugi, D. and Grossman, J.C. (2012) Water Desalination across Nanoporous
435 Graphene. Nano Letters 12(7), 3602-3608.

436 Elimelech, M., Chen, W.H. and Waypa, J.J. (1994) Measuring the zeta (electrokinetic)
437 potential of reverse osmosis membranes by a streaming potential analyzer. Desalination 95(3),
438 269-286.

439 Elimelech, M. and Phillip, W.A. (2011) The Future of Seawater Desalination: Energy,
440 Technology, and the Environment. Science 333(6043), 712-717.

441 Hancock, N.T. and Cath, T.Y. (2009) Solute Coupled Diffusion in Osmotically Driven
442 Membrane Processes. Environmental Science & Technology 43(17), 6769-6775.

443 Hancock, N.T., Phillip, W.A., Elimelech, M. and Cath, T.Y. (2011a) Bidirectional
444 Permeation of Electrolytes in Osmotically Driven Membrane Processes. Environmental
445 Science & Technology 45(24), 10642-10651.

446 Hancock, N.T., Xu, P., Heil, D.M., Bellona, C. and Cath, T.Y. (2011b) Comprehensive
447 Bench- and Pilot-Scale Investigation of Trace Organic Compounds Rejection by Forward
448 Osmosis. Environmental Science & Technology 45(19), 8483-8490.

449 Hoover, L.A., Phillip, W.A., Tiraferri, A., Yip, N.Y. and Elimelech, M. (2011) Forward with
450 Osmosis: Emerging Applications for Greater Sustainability. Environmental Science &
451 Technology 45(23), 9824-9830.

452 Jin, X., Shan, J., Wang, C., Wei, J. and Tang, C.Y. (2012a) Rejection of pharmaceuticals by
453 forward osmosis membranes. Journal of Hazardous Materials 227–228, 55-61.

454 Jin, X., She, Q., Ang, X. and Tang, C.Y. (2012b) Removal of boron and arsenic by forward
455 osmosis membrane: Influence of membrane orientation and organic fouling. Journal of
456 Membrane Science 389, 182-187.

457 McCutcheon, J.R. and Elimelech, M. (2008) Influence of membrane support layer
458 hydrophobicity on water flux in osmotically driven membrane processes. Journal of
459 Membrane Science 318(1-2), 458-466.

460 Mi, B. and Elimelech, M. (2008) Chemical and physical aspects of organic fouling of forward
461 osmosis membranes. Journal of Membrane Science 320(1–2), 292-302.

462 Ng, H.Y. and Elimelech, M. (2004) Influence of colloidal fouling on rejection of trace
463 organic contaminants by reverse osmosis. Journal of Membrane Science 244(1–2), 215-226.

464 Nghiem, L.D. and Hawkes, S. (2007) Effects of membrane fouling on the nanofiltration of
465 pharmaceutically active compounds (PhACs): Mechanisms and role of membrane pore size.
466 Separation and Purification Technology 57(1), 176-184.

467 Nghiem, L.D., Vogel, D. and Khan, S. (2008) Characterising humic acid fouling of
468 nanofiltration membranes using bisphenol A as a molecular indicator. Water Research 42(15),
469 4049-4058.

470 Parida, V. and Ng, H.Y. (2013) Forward osmosis organic fouling: Effects of organic loading,
471 calcium and membrane orientation. Desalination 312, 88-98.

472 Phillip, W.A., Yong, J.S. and Elimelech, M. (2010) Reverse Draw Solute Permeation in
473 Forward Osmosis: Modeling and Experiments. Environmental Science & Technology 44(13),
474 5170-5176.

475 Plakas, K.V., Karabelas, A.J., Wintgens, T. and Melin, T. (2006) A study of selected
476 herbicides retention by nanofiltration membranes—The role of organic fouling. Journal of
477 Membrane Science 284(1–2), 291-300.

478 Schwarzenbach, R.P., Escher, B.I., Fenner, K., Hofstetter, T.B., Johnson, C.A., von Gunten,
479 U. and Wehrli, B. (2006) The Challenge of Micropollutants in Aquatic Systems. Science
480 313(5790), 1072-1077.

481 Shaffer, D.L., Yip, N.Y., Gilron, J. and Elimelech, M. (2012) Seawater desalination for
482 agriculture by integrated forward and reverse osmosis: Improved product water quality for
483 potentially less energy. Journal of Membrane Science 415–416, 1-8.

484 Shannon, M.A., Bohn, P.W., Elimelech, M., Georgiadis, J.G., Marinas, B.J. and Mayes, A.M.
485 (2008) Science and technology for water purification in the coming decades. Nature
486 452(7185), 301-310.

487 Simon, A., Price, W. and Nghiem, L. (2011) Implications of membrane fouling toward the
488 removal of the pharmaceutical sulfamethoxazole by nanofiltration processes. Journal of
489 Zhejiang University SCIENCE A 12(8), 575-582.

490 Sutzkover, I., Hasson, D. and Semiat, R. (2000) Simple technique for measuring the
491 concentration polarization level in a reverse osmosis system. Desalination 131(1–3), 117-127.

492 Tang, C.Y., Chong, T.H. and Fane, A.G. (2011) Colloidal interactions and fouling of NF and
493 RO membranes: A review. Advances in Colloid and Interface Science 164(1–2), 126-143.

494 Valladares Linares, R., Yangali-Quintanilla, V., Li, Z. and Amy, G. (2011) Rejection of
495 micropollutants by clean and fouled forward osmosis membrane. Water Research 45(20),
496 6737-6744.

497 Vogel, D., Simon, A., Alturki, A.A., Bilitewski, B., Price, W.E. and Nghiem, L.D. (2010)
498 Effects of fouling and scaling on the retention of trace organic contaminants by a
499 nanofiltration membrane: The role of cake-enhanced concentration polarisation. Separation
500 and Purification Technology 73(2), 256-263.

501 Wang, Y., Combe, C. and Clark, M.M. (2001) The effects of pH and calcium on the diffusion
502 coefficient of humic acid. Journal of Membrane Science 183(1), 49-60.

503 Xie, M., Nghiem, L.D., Price, W.E. and Elimelech, M. (2012a) Comparison of the removal of
504 hydrophobic trace organic contaminants by forward osmosis and reverse osmosis. Water
505 Research 46(8), 2683-2692.

506 Xie, M., Price, W.E. and Nghiem, L.D. (2012b) Rejection of pharmaceutically active
507 compounds by forward osmosis: Role of solution pH and membrane orientation. Separation
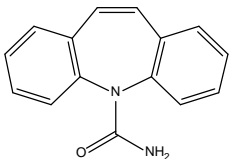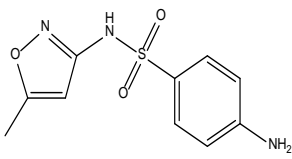508 and Purification Technology 93, 107-114.

509 Xu, P., Drewes, J.E., Kim, T.-U., Bellona, C. and Amy, G. (2006) Effect of membrane
510 fouling on transport of organic contaminants in NF/RO membrane applications. Journal of
511 Membrane Science 279(1–2), 165-175.

512 Yangali-Quintanilla, V., Li, Z., Valladares, R., Li, Q. and Amy, G. (2011) Indirect
513 desalination of Red Sea water with forward osmosis and low pressure reverse osmosis for
514 water reuse. Desalination 280(1-3), 160-166.

515 Yong, J.S., Phillip, W.A. and Elimelech, M. (2012) Coupled reverse draw solute permeation
516 and water flux in forward osmosis with neutral draw solutes. Journal of Membrane Science
517 392–393, 9-17.

518   Zhao, S., Zou, L., Tang, C.Y. and Mulcahy, D. (2012) Recent developments in forward
519   osmosis: Opportunities and challenges. Journal of Membrane Science 396, 1-21.

521 **Table 1**: Key physicochemical properties of model PhACs used in this study

Pharmaceutical		Carbamazepine	Sulfamethoxazole
Structure			
Molecular weight (Da)		236.3	253.3
pK_a [a]		9.73	1.7; 5.8
Log K_{ow} [a]		2.45	0.89
Molecular dimensions (nm) [b]	Length	0.891	1.031
	Width	0.529	0.587
	Depth	0.507	0.526

522 [a] From the SciFinder Scholar (ACS) database.
523 [b] Molecular dimensions were calculated using Molecular Modelling Pro Version 6.3.3
524 (Chem SW Inc.).

526   **Figure 1:** Reverse salt (NaCl) and hydrogen ion fluxes and the deposition of humic acid onto

527   the membrane surface as a function of calcium in the feed solution. The deposition of humic

528   acid was determined by mass balance calculation. The experimental conditions were as

529   follows: initial concentrations of carbamazepine and sulfamethoxazole in the feed = 500 µg/L,

530   initial concentration of humic acid = 50 mg/L, initial feed solution pH = 6.5, the background

531   electrolyte contained 20 mM NaCl, 1 mM NaHCO$_3$, and varying concentrations of Ca^{2+},

532   draw solution = 0.5 M NaCl, cross-flow rate = 1 L/min for both sides (corresponding to the

533   cross-flow velocity of 9 cm/s), and temperatures of the feed and draw solutions = 25 ± 1 °C.

534   Error bar represents standard deviation from duplicate runs at the specified experimental

535   conditions.

536   **Figure 2:** Pure water and salt (NaCl) permeability coefficients in clean and humic acid

537   matrices with calcium concentrations from 0 to 4 mM. Error bar represents standard deviation

538   from duplicate experiments.

539   **Figure 3:** The permeate water flux of humic acid fouling in forward osmosis (FO). FO

540   experimental conditions: the initial feed pH = 6.5 and the feed solution contained 50 mg/L

541   humic acid in a background electrolyte (20 mM NaCl, 1 mM NaHCO$_3$, and varying

542   concentrations of Ca^{2+} from 0 to 4 mM). Draw solution = 0.5 M NaCl. Cross-flow rate = 1

543   L/min (corresponding to the cross-flow velocity of 9 cm/s). Temperatures of feed and draw

544   solutions were 25 ± 1 °C.

545   **Figure 4:** Zeta potential of virgin and humic acid-fouled FO membranes. A humic acid-

546   fouled membrane was dried in a desiccator and then soaked in Milli-Q water for 24 hours

547   prior to the measurement. The humic acid fouling experimental conditions were described in

548   Figure 1. Error bar represents the standard deviation of duplicate measurements of two

549   membrane samples at the specified experimental conditions.

550   **Figure 5:** Permeation of carbamazepine and sulfamethoxazole in the clean matrix and in the

551   humic acid matrix at varying concentrations of Ca^{2+}. The experimental conditions were

552   described in Figure 1. The error bar represents the standard deviation from duplicate

553   experiments.

554   **Figure 6:** The flux of reverse draw solute and the deposition of humic acid in clean and

555   humic acid matrices using 0.5 M NaCl, 2.5 M MgSO$_4$, 3 M glucose, and 3.5 M urea as draw

556   solutions, respectively. The experimental conditions were as follows: the initial

557   concentrations of carbamazepine and sulfamethoxazole in the feed = 500 µg/L, initial feed

558   pH = 6.5, initial humic acid concentration = 50 mg/L, the background electrolyte solution

559   contained 20 mM NaCl, 1 mM NaHCO$_3$, and 2 mM Ca^{2+}. Varying draw solutions of 0.5 M

560   NaCl, 2.5 M MgSO$_4$, 3 M glucose, and 3.5 M urea were used to induce the same initial water

561   flux. The feed and draw solution temperature was 25 ± 1 °C. Cross-flow rate = 1 L/min for

562   both sides (corresponding to the cross-flow velocity of 9 cm/s).

563   **Figure 7:** Comparison of permeation of (a) sulfamethoxazole and (b) carbamazepine using

564   varying types and concentrations of draw solutes in FO. Other experimental conditions were

565   described in Figure 6.

566   **Figure 8:** Comparison of permeation of sulfamethoxazole and carbamazepine and reverse

567   salt (NaCl) flux among virgin membrane, humic acid fouled membrane, and physically

568   cleaned membrane at an initial feed pH of 6.5. Experimental conditions for the physically

569   cleaned membrane were: initial concentrations of sulfamethoxazole and carbamazepine in the

570   feed = 500 µg/L, initial pH = 6.5, the background electrolyte contained 20 mM NaCl and 1

571   mM NaHCO$_3$, draw solution = 0.5 M NaCl, cross-flow rate = 1 L/min for both sides

572   (corresponding to the cross-flow velocity of 9 cm/s), temperatures of the feed and draw
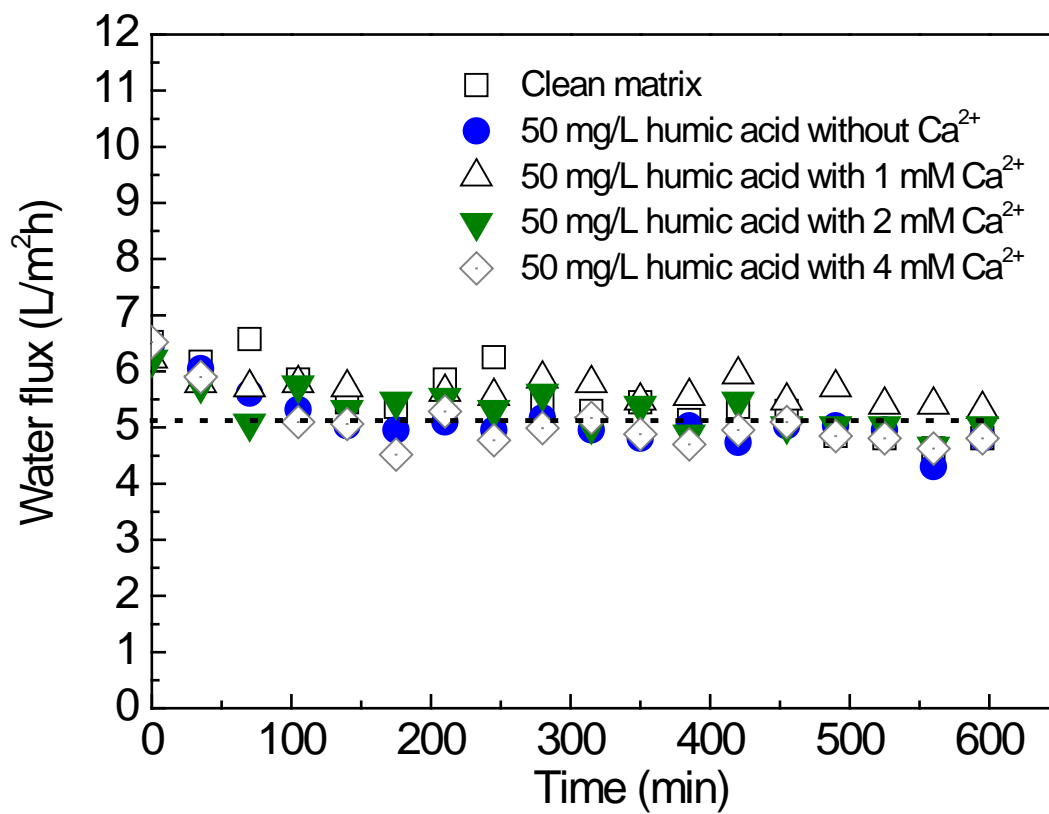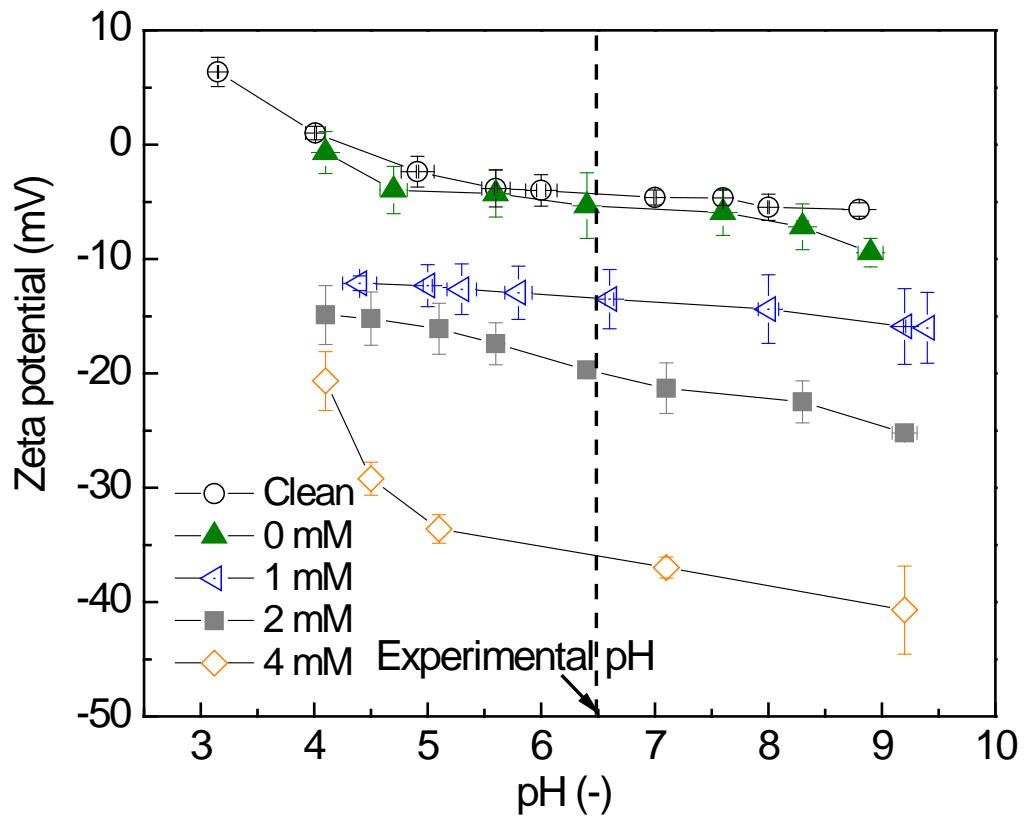
573   solutions = 25 ± 1 °C.
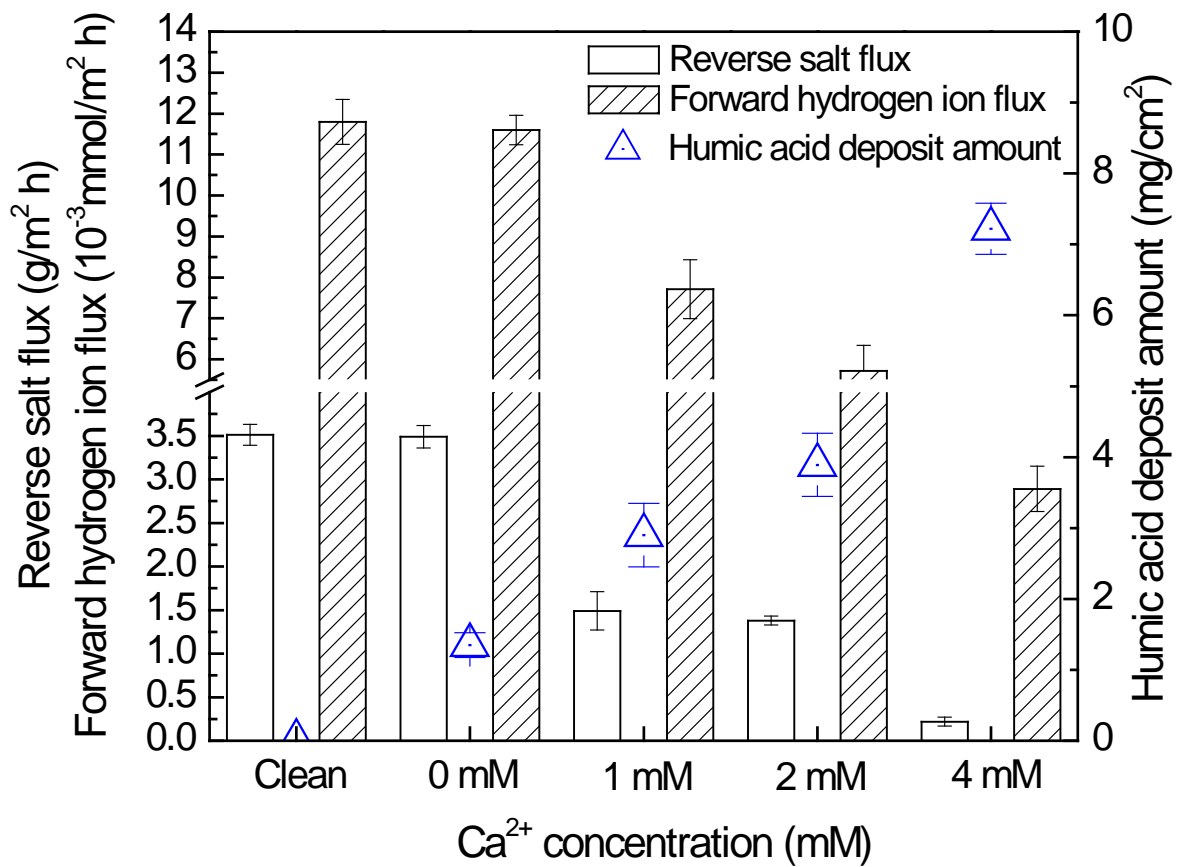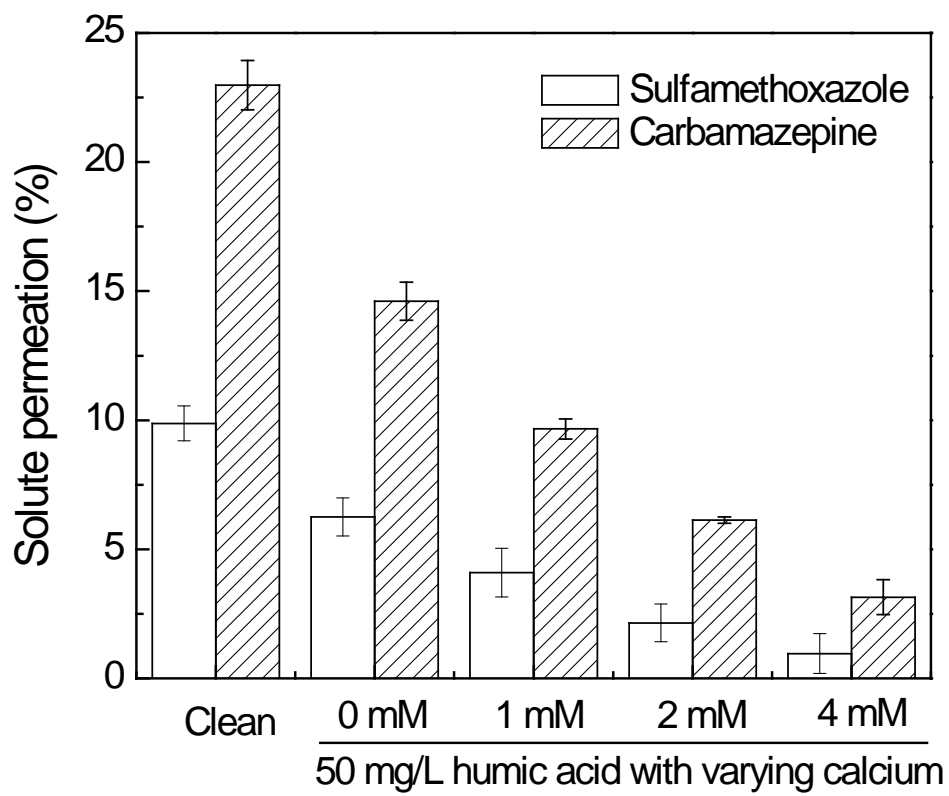
574

575   **Figure 1**
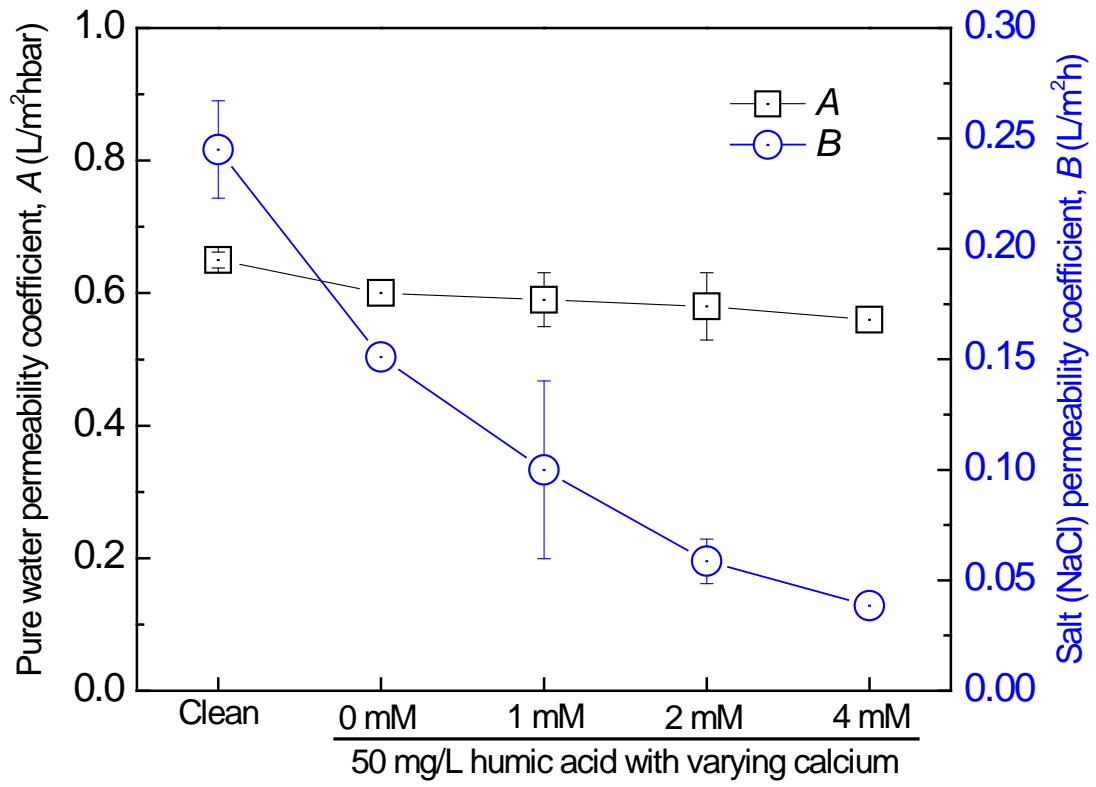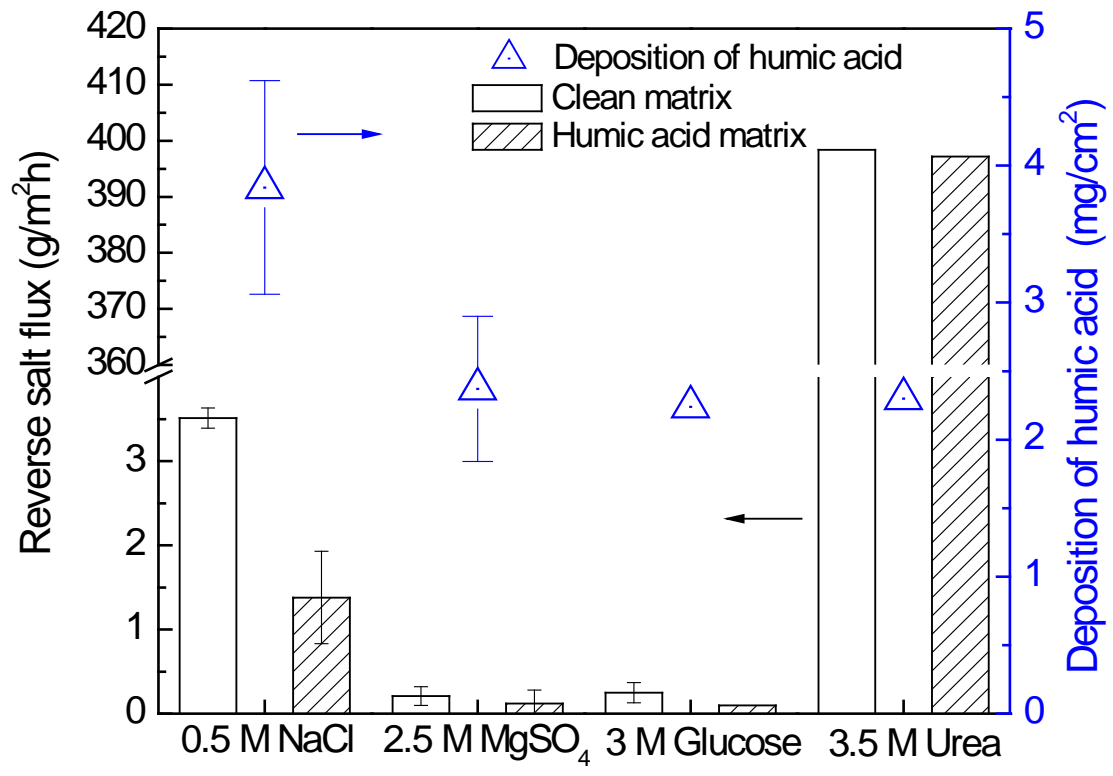
576
577 **Figure 2**
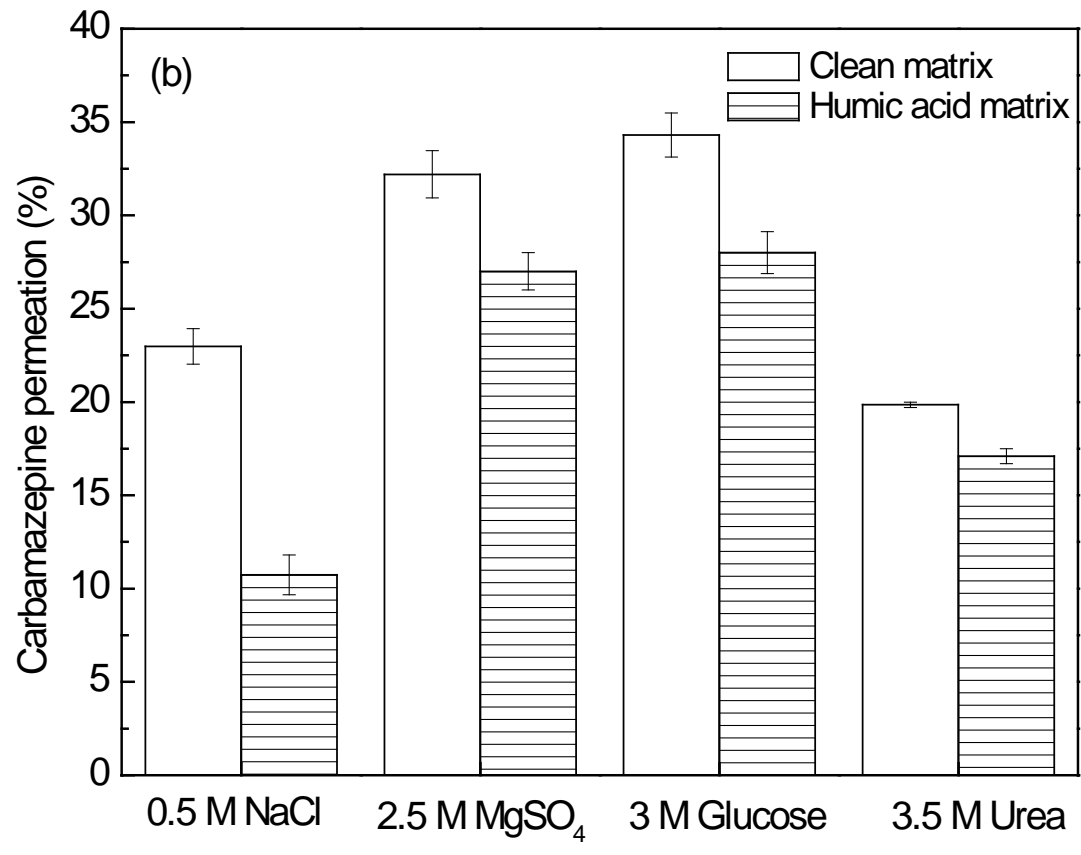
578

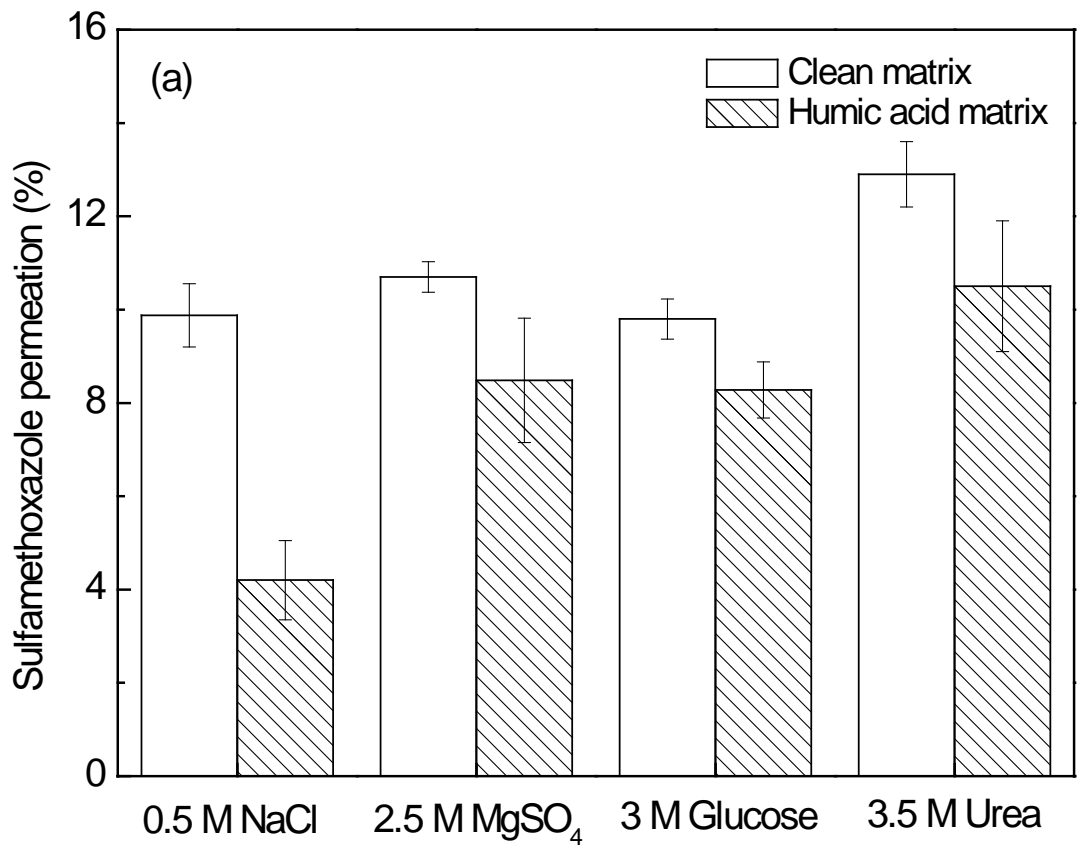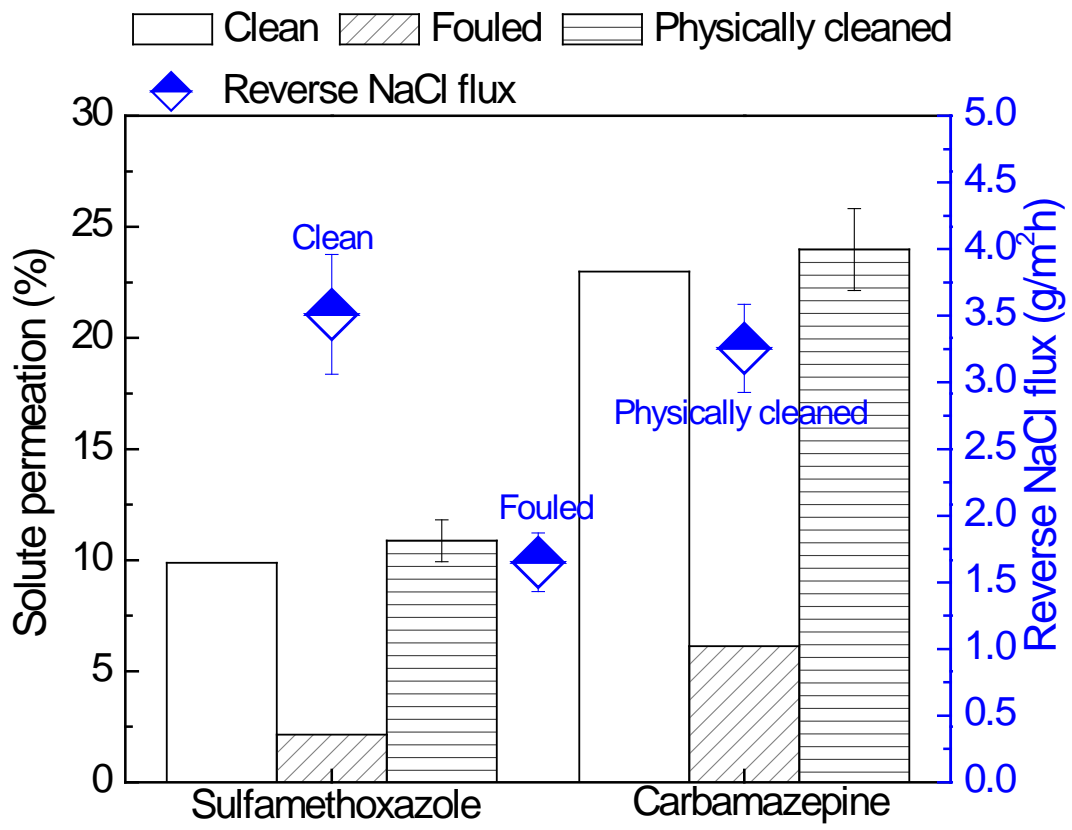579   **Figure 3**

580

581 **Figure 4**

582

583 **Figure 5**

584

585 **Figure 6**

586

Figure 7

588

589 **Figure 8**